Tracking-in-Formation of Multiple Autonomous Marine Vehicles under Proximity and Collision-Avoidance Constraints

Esteban Restrepo, Josef Matouš, Kristin y Pettersen

Tracking-in-Formation of Multiple Autonomous Marine Vehicles under Proximity and Collision-Avoidance Constraints

Esteban Restrepo, Josef Matouš, Kristin Pettersen

Tracking-in-Formation of Multiple Autonomous Marine Vehicles under Proximity and Collision-Avoidance Constraints

Esteban Restrepo Josef Matouš Kristin Y. Pettersen

***Abstract*— We propose a distributed control law that solves the tracking-in-formation problem for a group of underactuated autonomous marine vehicles interconnected over an undirected graph and subject to inter-agent collision-avoidance and connectivity constraints. The control approach is based on input-output feedback linearization using the so-called *hand-position* point as the output. Moreover, the control strategy is able to deal with limited knowledge on the target's state and dynamics as well as with disturbances in the form of unknown irrotational ocean currents. We establish *almost-everywhere* uniform asymptotic stability of the output dynamics with guaranteed respect of the inter-agent constraints. A numerical simulation illustrates the effectiveness of the proposed approach.**

I. INTRODUCTION

Formations of autonomous surface vehicles (ASVs) and underwater vehicles (AUVs) are used in a variety of applications, including ocean survey, marine biology, and oil and gas production [1]. In such applications, the vehicles typically follow a predefined trajectory while carrying sensor payloads to collect data from the environment. To accomplish their mission, the vehicles need to track the given trajectory while maintaining the desired formation shape.

Numerous methods have been proposed to solve the formation tracking problem. These methods include, among others, coordinated path-following [2], [3], optimal control [4], and leader-follower schemes [5], [6]. A comprehensive overview of these methods is presented in [7].

Due to the communication challenges posed by the underwater environment, the vehicles need to keep a sufficiently close distance to make the communication reliable. At the same time, the vehicles should keep a sufficiently large distance to avoid collisions. However, most of the methods in the literature do not simultaneously guarantee connectivity preservation and collision avoidance. Collision avoidance is typically handled by a reactive supervisory controller that intervenes when the vessel reaches the boundary of the *safe set* given by the constraints. Numerous reactive control algorithms, such as virtual potential fields [8], geometric guidance [9], and control barrier functions [10], have been proposed.

In the recent years, the so-called *edge-agreement* representation was proposed to solve the formation-keeping problem in a distributed manner [11]. This representation combined with *barrier Lyapunov functions* has been shown to achieve consensus under inter-agent constraints with guaranteed stability and robustness properties [12]. However, the results in [12] do not address the tracking and collision-avoidance problems. Moreover, the edge-agreement method cannot be directly applied to nonlinear nonholonomic dynamics. Hence, to make this method applicable to ASVs/AUVs, we use the *hand-position transformation* [13] to make the dynamics of the vehicles holonomic.

In this paper, we propose an edge-agreement based distributed control law for the tracking-in-formation problem that guarantees both connectivity preservation and collision avoidance. Our proposed approach is applicable to multiple ASVs or AUVs moving in the horizontal plane. We establish *almost everywhere* uniform asymptotic stability of the tracking-in-formation objective with guaranteed respect of the connectivity and collision-avoidance constraints. Moreover, we show that the output error dynamics converge to the origin exponentially fast.

II. MODEL AND PROBLEM FORMULATION

A. Model of the vessel

We consider a 3-DOF model representing the motion of an ASV or an AUV moving in the horizontal plane, see [14] for more details. First, the following assumptions are made.

Assumption 1: The motion of each vehicle is described in three degrees of freedom, *i.e.*, surge, sway, and yaw.

Assumption 2: The vehicles are port-starboard symmetric.

Assumption 3: The hydrodynamic damping is linear.

Assumption 4: The ocean current in the inertial frame $\mathbf{V} = [V_x \; V_y]^\top$ is constant, irrotational, and bounded, *i.e.*, $\exists V_{max} > 0$ such that $\sqrt{V_x^2 + V_y^2} \leq V_{\max}$.

Under these assumptions, for each vehicle i, the model in component form is

$$\dot{x}_i = u_{ri} \cos\psi_i - v_{ri} \sin\psi_i + V_x \tag{1a}$$
$$\dot{y}_i = u_{ri} \sin\psi_i + v_{ri} \cos\psi_i + V_y \tag{1b}$$
$$\dot{\psi}_i = r_i \tag{1c}$$
$$\dot{u}_{ri} = F_{u_r}(v_{ri}) + \tau_{ui} \tag{1d}$$
$$\dot{v}_{ri} = X(u_{ri}) r_i + Y(u_{ri}) v_{ri} \tag{1e}$$
$$\dot{u}_{ri} = F_r(u_{ri}, v_{ri}, r_i) + \tau_{ri} \tag{1f}$$

where $\eta_i := [x_i \; y_i \; \psi_i]^\top$ is the pose of each vehicle in the *North-East-Down* (NED) frame, $\nu_{ri} := [u_{ri} \; v_{ri} \; r_i]^\top$ are the relative (with respect to the ocean current) velocities in the body frame, surge velocity, sway velocity, and yaw rate,

E. Restrepo is with DTIS, ONERA, Université Paris-Saclay, F-91123 Palaiseau, France. esteban.restrepo@onera.fr. J. Matouš and K. Y. Pettersen are with the Centre for Autonomous Marine Operations and Systems, Department of Engineering Cybernetics, Norwegian University of Science and Technology (NTNU), Trondheim, Norway. {Josef.Matous, Kristin.Y.Pettersen}@ntnu.no

Manuscript 125 submitted to 2022 European Control Conference (ECC).
Received October 31, 2021.

respectively, and τ_{ui}, τ_{ri} are the control inputs. The functions F_{u_r}, F_r are given in Appendix I. Furthermore, $X(u_{ri}) = -X_1 u_{ri} + X_2$, $Y(u_{ri}) = -Y_1 u_{ri} - Y_2$, where X_1, X_2, Y_1, and Y_2 are given in Appendix I. Moreover, we make the following assumption:

Assumption 5: The following bounds hold on Y_1, Y_2:

$$Y_1 > 0, \quad Y_2 > 0.$$

Remark 1: Note that $Y_1, Y_2 > 0$ implies $Y(u_{ri}) < 0$. This is a natural assumption since $Y(u_{ri}) \geq 0$ corresponds to the situation of unstable sway dynamics. That is, a small perturbation applied along the sway direction would cause an undamped motion, which is unfeasible for commercial marine vehicles by design.

B. Hand-position transformation

The equations (1) are the dynamic model commonly used in the literature for the control of marine underactuated vehicles, where the output is normally chosen as the pivot point $p_i := [x_i \ y_i]^\top$ (the origin of the body-fixed frame). In what follows, we choose a different output, the so-called *hand-position point*, $h_i := [\xi_{1i} \ \xi_{2i}]^\top$, introduced in [13] for marine vehicles and defined as

$$\xi_{1i} := x_i + l\cos\psi_i, \quad \xi_{2i} := y_i + l\sin\psi_i, \tag{2}$$

where $l > 0$ is a constant, see Fig. 1 for the ASV case.

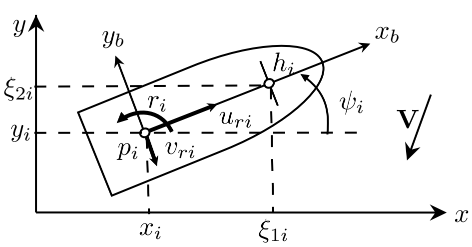

Fig. 1. Diagram of an ASV.

The use of the output h_i allows us to use an input-output feedback linearization of the model (1). More precisely, we define the change of coordinates

$$\zeta_{1i} = \psi_i \tag{3a}$$
$$\zeta_{2i} = r_i \tag{3b}$$
$$\xi_{1i} = x_i + l\cos\psi_i \tag{3c}$$
$$\xi_{2i} = y_i + l\sin\psi_i \tag{3d}$$
$$\xi_{3i} = u_{ri}\cos\psi_i - v_{ri}\sin\psi_i - r_i l\sin\psi_i \tag{3e}$$
$$\xi_{4i} = u_{ri}\sin\psi_i + v_{ri}\cos\psi_i + r_i l\cos\psi_i. \tag{3f}$$

The model (1) expressed in these new coordinates is then

$$\dot{\zeta}_{1i} = \zeta_{2i} \tag{4a}$$
$$\dot{\zeta}_{2i} = F_{\zeta_2}(\zeta_{1i}, \xi_{3i}, \xi_{4i}) + \tau_{ri} \tag{4b}$$
$$\begin{bmatrix}\dot{\xi}_{1i}\\ \dot{\xi}_{2i}\end{bmatrix} = \begin{bmatrix}\xi_{3i} + V_x\\ \xi_{4i} + V_y\end{bmatrix} \tag{4c}$$
$$\begin{bmatrix}\dot{\xi}_{3i}\\ \dot{\xi}_{4i}\end{bmatrix} = \begin{bmatrix}F_{\xi_3}(\zeta_{1i}, \xi_{3i}, \xi_{4i})\\ F_{\xi_4}(\zeta_{1i}, \xi_{3i}, \xi_{4i})\end{bmatrix} + \mathfrak{R}(\zeta_{1i})\begin{bmatrix}\tau_{ui}\\ l\tau_{ri}\end{bmatrix} \tag{4d}$$

where $F_{\zeta_2}(\zeta_{1i}, \xi_{3i}, \xi_{4i})$ is obtained from $F_r(u_{ri}, v_{ri}, r_i)$ substituting $u_{ri} = \xi_{3i}\cos\zeta_{1i} + \xi_{4i}\sin\zeta_{1i}$, $v_{ri} = -\xi_{3i}\sin\zeta_{1i} + \xi_{4i}\cos\zeta_{1i} - \zeta_{2i}l$, $r_i = \zeta_{2i}$,

$$\begin{bmatrix}F_{\xi_3}(\cdot)\\ F_{\xi_4}(\cdot)\end{bmatrix} = \mathfrak{R}(\psi_i)\begin{bmatrix}F_{u_r}(\cdot) - v_{ri}r_i - lr_i^2\\ u_{ri}r_i + X(\cdot)r_i + Y(\cdot)v_{ri} + F_r(\cdot)l\end{bmatrix}, \tag{5}$$

and $\mathfrak{R}(\cdot) \in \mathrm{SO}(2)$ denotes the rotation matrix.

Now, in order to linearize the external dynamics, we apply the input transformation

$$\begin{bmatrix}\tau_{ui}\\ l\tau_{ri}\end{bmatrix} = \mathfrak{R}(\psi_i)^\top \begin{bmatrix}-F_{\xi_3}(\zeta_{1i}, \xi_{3i}, \xi_{4i}) + \mu_{1i}\\ -F_{\xi_4}(\zeta_{1i}, \xi_{3i}, \xi_{4i}) + \mu_{2i}\end{bmatrix} \tag{6}$$

where μ_{1i}, μ_{2i} are the new inputs to be designed. Applying the input transformation (6) into (4), we obtain

$$\dot{\zeta}_{1i} = \zeta_{2i} \tag{7a}$$
$$\begin{aligned}\dot{\zeta}_{2i} = &-\left[\left(Y_1 - \frac{X_1 - 1}{l}\right)U_i\cos(\zeta_{1i} - \phi_i) + Y_2 + \frac{X_2}{l}\right]\zeta_{2i}\\ &-\left[\frac{Y_1}{l}U_i\cos(\zeta_{1i} - \phi_i) + \frac{Y_2}{l}\right]U_i\sin(\zeta_{1i} - \phi_i)\\ &-\frac{\sin\zeta_{1i}}{l}\mu_{1i} + \frac{\cos\zeta_{1i}}{l}\mu_{2i}\end{aligned} \tag{7b}$$
$$\dot{\xi}_{1i} = \xi_{3i} + V_x \tag{7c}$$
$$\dot{\xi}_{2i} = \xi_{4i} + V_y \tag{7d}$$
$$\dot{\xi}_{3i} = \mu_{1i} \tag{7e}$$
$$\dot{\xi}_{4i} = \mu_{2i} \tag{7f}$$

where

$$U_i = \sqrt{\xi_{3i}^2 + \xi_{4i}^2}, \quad \phi_i = \arctan 2\left(\frac{\xi_{4i}}{\xi_{3i}}\right). \tag{8}$$

The main advantage of choosing h_i as the output is that the nonlinear system (1) is transformed into (7) with the linear external dynamics (7c)-(7f). Note, however, that the inputs μ_{1i} and μ_{2i} affect also the internal dynamics (7a)-(7b). Therefore, the internal stability properties of the states ζ_{1i} and ζ_{2i} have to be verified.

C. Control objectives

It is assumed that each agent has access only to local information from a limited number of neighbors. This is represented by a graph, denoted $\mathcal{G} = (\mathcal{V}, \mathcal{E})$, where the set of nodes $\mathcal{V} := \{1, 2, \ldots, N\}$ corresponds to the labels of the agents and the set of edges $\mathcal{E} \subseteq \mathcal{V}^2$, of cardinality M, represents the communication between a pair of nodes. An edge e_k, $k \leq M$, is an ordered pair $(i, j) \in \mathcal{E}$ indicating that agent j has access to information from node i. In this paper we consider that the graph representing the interaction among the agents is undirected and connected, that is, there exists a path connecting each agent with every other agent.

We consider multi-agent systems that are subject to inter-agent constraints. For one part, these constraints come from the embedded relative-measurements devices, which are reliable only if used within a limited range. The vehicles must thus remain within a limited distance from their neighbors in order to maintain the connectivity of the graph. Moreover, to ensure the safety of the system, the agents must

Manuscript 125 submitted to 2022 European Control Conference (ECC).
Received October 31, 2021.

avoid collisions among themselves. These connectivity and collision-avoidance constraints may be defined as a set of restrictions on the system's output (2).

Define the relative-output state of a pair of interconnected agents as

$$z_{1k} := h_i - h_j \quad \forall k \leq M, \quad (i,j) \in \mathcal{E}. \tag{9}$$

For each $k \leq M$, let δ_k and Δ_k be, respectively, the minimal and maximal distances between agents i and j so that collisions are avoided and that the communication through edge e_k is reliable. Then, the set of inter-agent output constraints is defined as

$$\mathcal{D}_k := \left\{ z_{1k} \in \mathbb{R}^2 : \delta_k < |z_{1k}| < \Delta_k \right\}, \quad \forall\, k \leq M. \tag{10}$$

The control goal is for the agents to achieve a desired formation and track a target in the presence of the output constraints as given by the set $\mathcal{D}_k$ in (10). The target is modeled as a second-order integrator

$$\dot{h}_o = \nu_{ho}, \quad \dot{\nu}_{ho} = \mu_o(t), \tag{11}$$

where $h_o := [\xi_{1o}\ \xi_{2o}]^\top \in \mathbb{R}^2$ and $\nu_{ho} := [\xi_{3o}\ \xi_{4o}]^\top \in \mathbb{R}^2$ are, respectively, the (hand-)position and velocity of the target, and $\mu_o(t)$ is its acceleration. Moreover, we assume that the following holds.

Assumption 6: For all $t > 0$ there exist positive constants $\underline{\nu}_{ho}$, $\overline{\nu}_{ho}$, and $\overline{\mu}_o$ such that

$$\underline{\nu}_{ho} \leq |\nu_{ho}(t)| \leq \overline{\nu}_{ho}, \quad |\mu_o(t)| \leq \overline{\mu}_o. \tag{12}$$

Mathematically, the tracking-in-formation problem translates into making $\nu_{hi}(t) \to \nu_{ho}(t)$ for all $i \in \mathcal{V}$, where $\nu_{hi} := [\xi_{3i}\ \xi_{4i}]^\top$, and making $h_i(t) \to h_o(t)$ and $h_i(t) - h_j(t) \to z^d_{1k}$, or equivalently, $z_{1k} \to z^d_{1k}$ in the edge coordinates, where $z^d_{1k} \in \mathbb{R}^2$ denotes the desired relative position between a pair of neighboring agents i and j.

To address the formation part, instead of considering the states of each individual agent (the nodes of the graph), as is more common in the literature, we consider the variables defined in (9) which denote the states of the interconnection arcs in the graph. This corresponds to the so-called edge-agreement framework [11] and it has the advantage of recasting the consensus objective as the stabilization of the origin in error coordinates.

Let us denote the so-called incidence matrix of a graph by $E \in \mathbb{R}^{N\times M}$, which is a matrix with rows indexed by the nodes and columns indexed by the edges. Its (i,k)th entry is defined as follows: $[E]_{ik} := -1$ if i is the terminal node of edge e_k, $[E]_{ik} := 1$ if i is the initial node of edge e_k, and $[E]_{ik} := 0$ otherwise. Let $h^\top = \left[h_1^\top \cdots h_N^\top\right] \in \mathbb{R}^{2N}$ be the collection of the hand-position points of all the agents of the system. Then, the edge states in (9) satisfy

$$z_1 := [E^\top \otimes I_2] h \tag{13}$$

where $z_1^\top = [z_{11}^\top \cdots z_{1M}^\top]^\top \in \mathbb{R}^{2M}$, '$\otimes$' denotes the Kronecker product, and I_2 is the identity matrix. The formation error, in turn, is defined as

$$\tilde{z}_1 = [E^\top \otimes I_2] h - z_1^d, \tag{14}$$

where $z_1^{d\top} = [z_{11}^{d\top} \cdots z_{1M}^{d\top}] \in \mathbb{R}^{2M}$. Similarly, let $\nu_h^\top = \left[\nu_{hi}^\top \cdots \nu_{hN}^\top\right] \in \mathbb{R}^{2N}$ be the collection of the hand-position-point velocities. Then, in the edge coordinates we define

$$z_2 := [E^\top \otimes I_2] \nu_h. \tag{15}$$

For the tracking part of the problem, we consider the case that only one agent has access to the target's (hand-position) state, h_o and ν_{ho}, and knows an upper bound $\bar{\mu}_o$ on the target's acceleration. Hence, without loss of generality, label the agent that has access to the target's information as "1" and let an additional edge states be defined as

$$\tilde{z}_{1o} := h_1 - h_o - z^d_{1o}, \quad z_{2o} := \nu_{h1} - \nu_{ho}, \tag{16}$$

where $z^d_{1o} \in \mathbb{R}^2$ is a desired displacement with respect to the target.

Now, let $\mu_i := [\mu_{1i}\ \mu_{2i}]^\top$ and $\mu^\top = \left[\mu_1^\top \cdots \mu_N^\top\right] \in \mathbb{R}^{2N}$ be the collection of the inputs of all the agents of the system. Then, the control objective is to design μ such that

$$\lim_{t\to\infty} \tilde{z}_{1o}(t) = 0 \qquad \lim_{t\to\infty} z_{2o}(t) = 0 \tag{17a}$$

$$\lim_{t\to\infty} \tilde{z}_1(t) = 0 \qquad \lim_{t\to\infty} z_2(t) = 0. \tag{17b}$$

One advantage of considering the edge states rather than the node states is that it is possible to obtain an equivalent reduced system which is easier to analyze using stability theory. As observed in [11], using an appropriate labeling of the edges, the incidence matrix can be expressed as

$$E = [\, E_t \quad E_c \,] \tag{18}$$

where $E_t \in \mathbb{R}^{N\times(N-1)}$ denotes the full-column-rank incidence matrix corresponding to an arbitrary spanning tree $\mathcal{G}_t \subset \mathcal{G}$ and $E_c \in \mathbb{R}^{N\times(M-N+1)}$ represents the incidence matrix corresponding to the remaining edges not contained in $\mathcal{G}_t$. Moreover, defining

$$R := [\, I_{N-1} \quad T \,], \quad T := \left(E_t^\top E_t\right)^{-1} E_t^\top E_c \tag{19}$$

with I_{N-1} denoting the $N-1$ identity matrix, one obtains an alternative representation of the incidence matrix of the graph given by

$$E = E_t R. \tag{20}$$

The identity (20) is useful to derive a reduced-order dynamic model, cf. [11]. Now, correspondingly, the error edges' states may be split as

$$z_\iota = \left[z_{\iota t}^\top \ \ z_{\iota c}^\top\right]^\top \quad \iota := \{1, 2\} \tag{21}$$

where $z_{\iota t} \in \mathbb{R}^{n(N-1)}$ are the states corresponding to the edges of an arbitrary spanning tree $\mathcal{G}_t$ and $z_{\iota c} \in \mathbb{R}^{n(M-N+1)}$ denote the states of the remaining edges, $\mathcal{G}\backslash\mathcal{G}_t$. Thus, after (13), (14), (20), and (21), denoting $z^d_{1t} \in \mathbb{R}^{n(N-1)}$ as the vector of desired relative displacements corresponding to $\mathcal{G}_t$, we obtain

$$\tilde{z}_1 = \left[R^\top \otimes I_2\right] \tilde{z}_{1t}, \quad z_2 = \left[R^\top \otimes I_2\right] z_{2t}. \tag{22}$$

Now, the reduced-order external dynamics becomes

$$\dot{\tilde{z}}_{1o} = z_{2o} + \mathbf{V} \tag{23a}$$

$$\dot{\tilde{z}}_{1t} = z_{2t} \tag{23b}$$

Manuscript 125 submitted to 2022 European Control Conference (ECC).
Received October 31, 2021.

$$\dot{z}_{2o} = \mu_1 - \mu_o(t) \tag{23c}$$
$$\dot{z}_{2t} = \left[E_t^\top \otimes I_2\right]\mu. \tag{23d}$$

In these coordinates, the control objective as defined in (17) is achieved if and only if the origin of the reduced-order system (23) is asymptotically stabilized. More precisely, we consider the following problem.

Tracking-in-formation with inter-agent constraints: Consider a system of N autonomous marine vehicles with dynamics given by (1), interacting over an initially connected undirected graph. Assume, in addition, that the agents are subject to inter-agent constraints that consist in the outputs (2) being restricted to remain in the set defined in (10). Under these conditions, find distributed controllers μ_i, $i \leq N$, that achieve the objective (17) and render the set (10) forward invariant, *i.e.*, $z_{1k}(0) \in \mathcal{D}_k$ implies that $z_{1k}(t) \in \mathcal{D}_k$, $\forall k \leq M$ and $\forall t \geq 0$.

III. Control design

In this section we will show how the tracking-in-formation problem, with the previously formulated output constraints, can be solved following a backstepping approach, which is well adapted to the normal form of the external dynamics (23). We start by defining a virtual control law for (23a)-(23b) with z_{2o} and z_{2t} as inputs. Now, in order to account for the output constraints, a good choice of control design for the virtual inputs consists in using the gradient of a *barrier Lyapunov function* [12], [15], [16].

Barrier Lyapunov functions (BLFs) are reminiscent of Lyapunov functions, so they are positive definite, but their domain of definition is restricted by design to open subsets of the Euclidean space. Furthermore, they grow unbounded as z_{1k} approaches the boundary of their domain. We define them as follows, cf. [17].

Definition 1 (BLF): Consider the system $\dot{x} = f(x)$ and let $\mathcal{M}$ be an open set containing the origin. A BLF is a positive definite function $V : \mathcal{M} \to \mathbb{R}_{\geq 0}$, $x \mapsto V(x)$, that is $\mathcal{C}^1$, satisfies

$$\nabla V(x)^\top f(x) := \frac{\partial V(x)}{\partial x}^\top f(x) \leq 0,$$

and has the property that $V(x) \to \infty$ and $|\nabla V(x)| \to \infty$ as $x \to \partial\mathcal{M}$.

Akin to (10), the inter-agent constraints in terms of the formation error are given by the set

$$\tilde{\mathcal{D}}_k := \{\tilde{z}_{1k} \in \mathbb{R}^2 \,:\, \delta_k < |\tilde{z}_{1k} + z_{1k}^d| < \Delta_k\}, \quad \forall k \leq M. \tag{24}$$

Then, for each $k \leq M$, we define a candidate BLF $W_k : \tilde{\mathcal{D}}_k \to \mathbb{R}_{\geq 0}$, of the form

$$W_k(\tilde{z}_{1k}) = \frac{1}{2}\left[|\tilde{z}_{1k}|^2 + B_k(\tilde{z}_{1k} + z_{1k}^d)\right], \tag{25}$$

where

$$B_k(z_{1k}) = \kappa_{1k}\left[\ln\left(\frac{\Delta_k^2}{\Delta_k^2 - |z_{1k}|^2}\right) - \ln\left(\frac{\Delta_k^2}{\Delta_k^2 - |z_{1k}^d|^2}\right)\right] + \kappa_{2k}\left[\ln\left(\frac{|z_{1k}|^2}{|z_{1k}|^2 - \delta_k^2}\right) - \ln\left(\frac{|z_{1k}^d|^2}{|z_{1k}^d|^2 - \delta_k^2}\right)\right],$$

$$\kappa_{1k} := \frac{\delta_k^2}{|z_{1k}^d|^2(|z_{1k}^d|^2 - \delta_k^2)}, \quad \kappa_{2k} := \frac{1}{\Delta_k^2 - |z_{1k}^d|^2}.$$

Note that B_k is a non-negative function that satisfies: $B_k(z_{1k}^d) = 0$, $\nabla B_k(z_{1k}^d) = 0$, and $B_k(\tilde{z}_{1k} + z_{1k}^d) \to \infty$ as either $|\tilde{z}_{1k} + z_{1k}^d| \to \Delta_k$ or $|\tilde{z}_{1k} + z_{1k}^d| \to \delta_k$. Therefore, the candidate BLF (25) satisfies: $W_k(\tilde{z}_{1k}) \to \infty$ as either $|\tilde{z}_{1k} + z_{1k}^d| \to \Delta_k$ or $|\tilde{z}_{1k} + z_{1k}^d| \to \delta_k$.

Remark 2: The functions defined in (25) are reminiscent of scalar potential functions in constrained environments. Hence, the appearance of multiple critical points is inevitable [18]. Indeed, the gradient of the BLF (25), $\nabla W_k(\tilde{z}_{1k})$, vanishes at the origin and at an isolated saddle point separated from the origin. Therefore, when using the gradient of (25), the closed-loop system has multiple equilibria. We will address such technical difficulties using tools tailored for so-called *multi-stable* systems, see [19], [20].

Now, we define a BLF for the multi-agent system as

$$W(\tilde{z}_{1t}) = \sum_{k \leq M} W_k(\tilde{z}_{1k}) \tag{26}$$

and, in light of Remark 2, let us denote by $\tilde{z}_1^* \in \mathbb{R}^{n(N-1)}$ the vector containing the saddle points of the BLF for each edge (25). Moreover, let us define the disjoint set

$$\mathcal{W} := \{0\} \cup \{\tilde{z}_1^*\}, \tag{27}$$

which corresponds to the critical points of W in (25). Then, W satisfies

$$\frac{a_1}{2}|\tilde{z}_{1t}|_{\mathcal{W}}^2 \leq W(\tilde{z}_{1t}) \leq a_2|\nabla W(\tilde{z}_{1t})|^2, \tag{28}$$

where $a_1, a_2 > 0$ and $|\tilde{z}_{1t}|_{\mathcal{W}} := \min\left\{|\tilde{z}_{1t}|, |\tilde{z}_{1t} - \tilde{z}_1^*|\right\}$.

In the edge-agreement framework, the BLF-based virtual controllers are then given by

$$z_{2t}^* = [E_t^\top \otimes I_2]\nu_h^*$$
$$\nu_h^* := -c_1[E_t \otimes I_2]\nabla W(\tilde{z}_{1t}) - c_1[C \otimes I_2]\tilde{z}_{1o} - \hat{V}, \tag{29}$$

where c_1 is a positive gain, $\hat{V}$ is a vector of estimates of the ocean current for each agent, and $C^\top := \begin{bmatrix} 1 & 0_{1\times(N-1)}^\top \end{bmatrix}$. Defining the error coordinates $\tilde{z}_{2t} := z_{2t} - z_{2t}^*$, $\tilde{z}_{2o} := \tilde{z}_{21} - z_{2o}$, and using (29), (23a)-(23b) become

$$\begin{bmatrix} \dot{\tilde{z}}_{1o} \\ \dot{\tilde{z}}_{1t} \end{bmatrix} = -c_1\left[\begin{bmatrix} 1 & C^\top E_t \\ E_t^\top C & E_t^\top E_t \end{bmatrix} \otimes I_2\right]\begin{bmatrix} \tilde{z}_{1o} \\ \nabla W(\tilde{z}_{1t}) \end{bmatrix} + \left[\begin{bmatrix} C^\top \\ E_t^\top \end{bmatrix} \otimes I_2\right]\tilde{V} + \begin{bmatrix} \tilde{z}_{2o} \\ \tilde{z}_{2t} \end{bmatrix} \tag{30}$$

where the estimation error $\tilde{V}$ is defined as

$$\tilde{V} := \left[I_N \otimes \begin{bmatrix} V_x & 0 \\ 0 & V_y \end{bmatrix}\right]\mathbf{1}_{2N} - \hat{V} = \bar{\mathbf{V}} - \hat{V}. \tag{31}$$

With aim at making $\tilde{V} \to 0$, we design the adaptation law

$$\hat{V} = c_v\left(h - \varphi\right), \quad c_v > 0 \tag{32a}$$
$$\dot{\varphi} = \nu_h + \hat{V}. \tag{32b}$$

Using (32) and (1c)-(1d), the derivative of (31) becomes

$$\dot{\tilde{V}} = -c_v\left(\nu_h + \bar{\mathbf{V}} - \nu_h - \hat{V}\right) = -c_v\tilde{V}. \tag{33}$$

Manuscript 125 submitted to 2022 European Control Conference (ECC).
Received October 31, 2021.

Now, we rewrite (23c)-(23d) in the error coordinates, $\tilde{z}_{2o}$ and $\tilde{z}_{2t}$:

$$\dot{\tilde{z}}_{2o} = \mu_1 - \dot{\nu}^*_{h1} \tag{34a}$$
$$\dot{\tilde{z}}_{2t} = \left[E_t^\top \otimes I_2\right]\mu - \dot{z}^*_{2t}. \tag{34b}$$

The tracking-in-formation control law is chosen as

$$\begin{aligned}\mu = &- c_2\left[E_t RR^\top \otimes I_2\right]\tilde{z}_{2t} - c_2[C \otimes I_2]\tilde{z}_{2o} + \dot{\bar{\nu}}^*_h \\ &- \gamma\text{sign}\left(\left[E_t RR^\top \otimes I_2\right]\tilde{z}_{2t} + [C \otimes I_2]\tilde{z}_{2o}\right)\end{aligned} \tag{35}$$

where $c_2, \gamma > 0$ and $\bar{\nu}^*_h = -c_1[E_t \otimes I_2]\nabla W(\tilde{z}_{1t}) - c_1[C \otimes I_2]\tilde{z}_{1o}$.

IV. Main result

First we assume that the following holds.

Assumption 7: The total relative velocity of the target is such that $U_o(t) = \sqrt{(\xi_{3o}(t) - V_x)^2 + (\xi_{4o}(t) - V_y)^2} > 0$.

Remark 3: Note that Assumptions 4 and 6 imply that there exist constants $\underline{U}_o$, $\overline{U}_o$, $\underline{U}^*_o$, and $\overline{U}^*_o$, such that $\underline{U}_o \leq U_o(t) \leq \overline{U}_o$ and $\underline{U}^*_o \leq \dot{U}_o(t) \leq \overline{U}^*_o$ for all $t > 0$.

Moreover, let us define the following variables:

$$a = \left(Y_1 - \frac{X_1 - 1}{l}\right)U_o, \qquad b = Y_2 + \frac{X_2}{l} \tag{36}$$
$$c = \frac{Y_1 U_o^2}{l}, \qquad d = \frac{Y_2 U_o}{l}. \tag{37}$$

Note that from Remark 3 we have that $\underline{a} \leq a \leq \overline{a}$, $\underline{c} \leq c \leq \overline{c}$, and $\underline{d} \leq d \leq \overline{d}$, with $\underline{a}, \overline{a}, \underline{c}, \overline{c}, \underline{d}, \overline{d}$ being positive constants.

Then, our main result is stated as follows.

Proposition 1: Consider N ASVs/AUVs, each described by the model (1), and interconnected over an initially connected undirected graph. Consider the hand-position point $h_i := [\xi_{1i}\ \xi_{2i}]^\top = [x_i + l\cos\psi_i\ y_i + l\sin\psi_i]^\top$, where $[x_i\ y_i]^\top$ is the position of the pivot point of the ith agent, $l > 0$ is a positive, and ψ_i is the yaw angle of the ith vehicle. Let $\phi_o(t) = \arctan(\xi_{4o}(t) - V_y/\xi_{3o}(t) - V_x)$ be the crab angle of the target. If Assumptions 1-7 are satisfied and if

$$0 < \bar{U}_o < \frac{Y_2}{Y_1}, \quad l > \max\left\{\frac{m_{22}}{m_{33}}, -\frac{X_2}{Y_2}\right\} \tag{38}$$
$$\gamma \geq \sqrt{2N}\mu_o \tag{39}$$
$$\bar{U}^*_o \leq \frac{2\min\{\underline{a}(\underline{d} - \underline{c}), b\}}{\frac{Y_1\bar{U}_o}{l} + 2\left(Y_1 - \frac{X_1 - 1}{l}\right)}, \tag{40}$$

the controller (6), where the new inputs μ_{1i} and μ_{2i} are given by (35), renders the constraints set (10) forward invariant and guarantees the achievement of the tracking-in-formation objective (17) for almost all initial conditions such that $z_{1k}(0) \in \mathcal{D}_k$, for all $k \leq M$. $\square$

Proof: We begin by rewriting the N systems (7) in closed loop with the new inputs (35) in a cascaded form. For that purpose let us define the error variables

$$\tilde{\zeta}_{1i} := \zeta_{1i} - \phi_o(t), \quad \tilde{\zeta}_{2i} := \zeta_{2i} - \dot{\phi}_o(t). \tag{41}$$

Moreover, define the tracking errors

$$\bar{\xi}_{3i} := \xi_{3i} - (\xi_{3o}(t) - V_x), \quad \bar{\xi}_{4i} := \xi_{4i} - (\xi_{4o}(t) - V_y). \tag{42}$$

Denote $\tilde{\zeta}_1^\top := \left[\tilde{\zeta}_{11} \cdots \tilde{\zeta}_{1N}\right]$, $\tilde{\zeta}_2^\top := \left[\tilde{\zeta}_{21} \cdots \tilde{\zeta}_{2N}\right]$, $\tilde{\zeta}^\top := \left[\tilde{\zeta}_1^\top\ \ \tilde{\zeta}_2^\top\right]$, $\bar{\nu}_{hi}^\top := \left[\bar{\xi}_{3i}\ \ \bar{\xi}_{4i}\right]$, $\bar{\nu}_h^\top := \left[\bar{\nu}_{h1}^\top \cdots \bar{\nu}_{hN}^\top\right]$, $\text{Sin}(\tilde{\zeta}_1)^\top := \left[\sin\tilde{\zeta}_{11} \cdots \sin\tilde{\zeta}_{1N}\right]$. Then, the internal dynamics for the whole multi-agent system in compact form can be rewritten as

$$\dot{\tilde{\zeta}}_1 = \tilde{\zeta}_2 \tag{43a}$$
$$\begin{aligned}\dot{\tilde{\zeta}}_2 = &- A(\tilde{\zeta})\tilde{\zeta}_2 - B(\tilde{\zeta})\text{Sin}(\tilde{\zeta}_1) + \bar{A}(\tilde{\zeta}, \bar{\nu}_h)\bar{\nu}_h + \bar{B}(\zeta_1)\mu \\ &- A(\tilde{\zeta})\mathbf{1}_N\dot{\phi}_o(t) - \mathbf{1}_N\ddot{\phi}_o(t)\end{aligned} \tag{43b}$$

where

$$A(\tilde{\zeta}) := \text{diag}\{a\cos\tilde{\zeta}_{1i} + b\},\ B(\tilde{\zeta}) := \text{diag}\{c\cos\tilde{\zeta}_{1i} + d\} \tag{44}$$

$$\bar{A}(\tilde{\zeta}, \bar{\nu}_h) := \text{blockdiag}\left\{\left[\alpha(\tilde{\zeta}_i, \bar{\xi}_{3i}, \bar{\xi}_{4i})\ \ \beta(\tilde{\zeta}_i, \bar{\xi}_{3i}, \bar{\xi}_{4i})\right]\right\} \tag{45}$$

$$\bar{B}(\zeta_1) := \text{blockdiag}\{[-\sin\zeta_{1i}\ \ \cos\zeta_{1i}]\}, \tag{46}$$

and $\alpha(\tilde{\zeta}_i, \bar{\xi}_{3i}, \bar{\xi}_{4i})$, $\beta(\tilde{\zeta}_i, \bar{\xi}_{3i}, \bar{\xi}_{4i})$ given in Appendix I. Now, defining $\chi^\top := \left[\tilde{z}_{1o}\ \ \tilde{z}_{1t}^\top\ \ \bar{\nu}_h^\top\ \ \tilde{V}^\top\right]$, the closed loop system takes the form

$$\dot{\tilde{\zeta}} = -H(\tilde{\zeta})\tilde{\zeta}_s + \Psi(t, \tilde{\zeta}) + G(\tilde{\zeta}, \chi) \tag{47a}$$
$$\dot{\chi} = F(t, \chi), \tag{47b}$$

where $\tilde{\zeta}_s^\top := \left[\text{Sin}(\tilde{\zeta}_1)^\top\ \ \tilde{\zeta}_2^\top\right]$,

$$H(\tilde{\zeta}) = \begin{bmatrix} 0 & I_N \\ B(\tilde{\zeta}) & A(\tilde{\zeta}) \end{bmatrix},\ F(t, \chi) = \begin{bmatrix} \bar{\nu}_{h1} \\ \left[E^\top \otimes I_2\right]\bar{\nu}_h \\ \mu - \mathbf{1}_N\mu_o(t) \\ -c_v\tilde{V} \end{bmatrix} \tag{48}$$

$$G(\tilde{\zeta}, \chi) = \begin{bmatrix} 0 \\ \bar{A}(\tilde{\zeta}, \bar{\nu}_h)\bar{\nu}_h + \bar{B}(\zeta_1)\mu \end{bmatrix} \tag{49}$$

$$\Psi(t, \tilde{\zeta}) = \begin{bmatrix} 0 \\ -A(\tilde{\zeta})\dot{\phi}_o(t) - \mathbf{1}_N\ddot{\phi}_o(t) \end{bmatrix}. \tag{50}$$

The stability analysis of the closed-loop cascaded system (47) follows a similar reasoning as in [13]. First, we show that the driving system (47b) is (almost-everywhere) uniformly asymptotically stable with domain of attraction corresponding to the set of constraints, and that its trajectories converge exponentially to the origin. Next, under the property that the trajectories of the external dynamics converge to the origin exponentially fast, it may be shown that the trajectories of the internal dynamics (47a) are uniformly globally ultimately bounded.

A. External dynamics

In order to analyze the stability properties of the subsystem (47b) we use the reduced-order edge-based system presented above. Let $\varsigma_1^\top = \left[\tilde{z}_{1o}\ \ \nabla\tilde{z}_{1t}^\top\right]$, $\bar{\varsigma}_1^\top = \left[\tilde{z}_{1o}\ \ \nabla W(\tilde{z}_{1t})^\top\right]$, $\varsigma_2^\top = \left[\tilde{z}_{2o}\ \ \tilde{z}_{2t}^\top\right]$, and

$$\mathcal{L} = \left[\begin{bmatrix} 1 & C^\top E_t \\ E_t^\top C & E_t^\top E_t \end{bmatrix} \otimes I_2\right] \tag{51}$$

$$\mathcal{R}_1 = \left[\begin{bmatrix} C^\top \\ E_t^\top \end{bmatrix} \otimes I_2\right],\ \mathcal{R}_2 = \left[\begin{bmatrix} 1 & 0_{(N-1)}^\top \\ 0_{(N-1)} & RR^\top \end{bmatrix} \otimes I_2\right]. \tag{52}$$

Manuscript 125 submitted to 2022 European Control Conference (ECC).
Received October 31, 2021.

Then, from (30), (34), and (35), the compact external dynamics in the edge-based perspective becomes

$$\dot{\varsigma}_1 = - c_1\mathcal{L}\bar{\varsigma}_1 + \varsigma_2 + \mathcal{R}_1\tilde{V} \tag{53a}$$

$$\begin{aligned}\dot{\varsigma}_2 = &- c_2\mathcal{L}\mathcal{R}_2\varsigma_2 + c_v\mathcal{R}_1\tilde{V} \\ &- \gamma\mathcal{R}_1\mathrm{sign}\left(\mathcal{R}_1^\top\mathcal{R}_2\varsigma_2\right) - \mathcal{R}_1\mathbf{1}_{2N}\mu_o(t)\end{aligned} \tag{53b}$$

$$\dot{\tilde{V}} = - c_v\tilde{V} \tag{53c}$$

Remark 4: The matrix $E_t^\top E_t$ represents the edge Laplacian of a spanning tree, therefore it is symmetric positive definite [11]. Then, taking the Schur complement of $E_t^\top E_t$ in (51), from the structure of C, we have that

$$1 - C^\top E_t(E_t^\top E_t)^{-1}E_t^\top C > 0. \tag{54}$$

Hence, from the positive-definiteness of $E_t^\top E_t$ and (54), the matrix $\mathcal{L}$ in (51) is positive definite.

For system (53) we state the following.

Lemma 1: The origin of the edge-based closed-loop system (53) is *almost-everywhere* uniformly asymptotically stable with domain of attraction $\mathbb{D} := \mathbb{R} \times \tilde{\mathcal{D}} \times \mathbb{R} \times \mathbb{R}^{2M} \times \mathbb{R}^{2N}$, with $\tilde{\mathcal{D}} := \bigcap_{k\leq M}\tilde{\mathcal{D}}_k$, where $\tilde{\mathcal{D}}_k$ is defined in (24). Furthermore, for almost all initial conditions, the trajectories of the closed-loop external dynamics (53) converge to the origin exponentially. □

Proof: First define the function

$$W_1(\varsigma_1) := \frac{1}{2}|\tilde{z}_{1o}|^2 + W(\tilde{z}_{1t}) \tag{55}$$

where $\tilde{z}_{1t} \mapsto W(\tilde{z}_{1t})$ is defined in (26). The derivative of (55) along the trajectories of (53a) yields

$$\dot{W}_1(\varsigma_1) = -c_1\bar{\varsigma}_1^\top\mathcal{L}\bar{\varsigma}_1 + \bar{\varsigma}_1^\top\varsigma_2 + \bar{\varsigma}_1^\top\mathcal{R}_1\tilde{V}, \tag{56}$$

and since $\mathcal{L}$ is positive definite, see Remark 4, (56) satisfies

$$\dot{W}_1(\varsigma_1) \leq -c_1'|\bar{\varsigma}_1|^2 + |\bar{\varsigma}_1||\varsigma_2| + c_v'|\bar{\varsigma}_1||\tilde{V}|, \tag{57}$$

where $c_1' := c_1\lambda_{\min}(\mathcal{L})$ and $c_v' := c_v|\mathcal{R}_1|$.

Next, define the candidate Lyapunov function

$$W_2(\varsigma_2) := \frac{1}{2}\varsigma_2^\top\mathcal{R}_2\varsigma_2 \tag{58}$$

We proceed by calculating the derivative of (58) along the trajectories of (53b), which is defined by the differential inclusion $\varsigma_2 \in F_2(t,\varsigma_2)$, where

$$F_2(t,\varsigma_2) := \begin{cases}\text{(53b)}, & \mathcal{R}_1^\top\mathcal{R}_2\varsigma_2 \neq 0 \\ -c_2\mathcal{L}\mathcal{R}_2\varsigma_2 + c_v\mathcal{R}_2\tilde{V} & \\ -\gamma\lambda - \mathcal{R}_2\mathbf{1}_{2N}\mu_o(t), & \mathcal{R}_1^\top\mathcal{R}_2\varsigma_2 = 0\end{cases} \tag{59}$$

and $\lambda \in [-1,1]$. Thus, using condition (39) and $||s||_1 = s^\top\mathrm{sign}(s)$, the derivative of W_2 yields

$$\begin{aligned}\dot{W}_2(\varsigma_2) = &-c_2\varsigma_2^\top\mathcal{R}_2\mathcal{L}\mathcal{R}_2\varsigma_2 + c_v\varsigma_2^\top\mathcal{R}_2\mathcal{R}_1\tilde{V} \\ &- \gamma\varsigma_2^\top\mathcal{R}_2\mathcal{R}_1\mathrm{sign}\left(\mathcal{R}_1^\top\mathcal{R}_2\varsigma_2\right) - \varsigma_2^\top\mathcal{R}_2\mathcal{R}_1\mathbf{1}_{2N}\mu_o(t) \\ &\leq -c_2'|\varsigma_2|^2 + c_v''|\varsigma_2||\tilde{V}|,\end{aligned} \tag{60}$$

where $c_2' := c_2\lambda_{\min}(\mathcal{R}_2\mathcal{L}\mathcal{R}_2)$ and $c_v'' := c_v|\mathcal{R}_2\mathcal{R}_1|$.

Next, let $\varsigma^\top := \begin{bmatrix}\varsigma_1^\top & \varsigma_2^\top & \tilde{V}^\top\end{bmatrix}$ and define the candidate Lyapunov function

$$W_\varsigma(\varsigma) := W_1(\varsigma_1) + \kappa_1W_2(\varsigma_2) + \frac{\kappa_2}{2}|\tilde{V}|^2. \tag{61}$$

From (57), (60), and (53c), we have

$$\begin{aligned}\dot{W}_\varsigma(\varsigma) \leq &- c_1'|\bar{\varsigma}_1|^2 - \kappa_1c_2'|\varsigma_2|^2 - \kappa_2c_v|\tilde{V}|^2 \\ &+ |\bar{\varsigma}_1||\varsigma_2| + c_v'|\varsigma_1||\tilde{V}| + \kappa_1c_v''|\varsigma_2||\tilde{V}|.\end{aligned} \tag{62}$$

Setting κ_1, κ_2 large enough, we obtain

$$\begin{aligned}\dot{W}_\varsigma(\varsigma) \leq &- \bar{c}_1|\bar{\varsigma}_1|^2 - \bar{c}_2|\varsigma_2|^2 - \bar{c}_v|\tilde{V}|^2 \\ \leq &- \bar{c}\,W_\varsigma(\varsigma).\end{aligned} \tag{63}$$

Now, recalling Remark 2, let

$$\mathcal{W}_\varsigma := \{0\} \times \mathcal{W} \times \{0\} \times \{0\}^{2(N-1)} \times \{0\}^{2N} \tag{64}$$

where $\mathcal{W}$ is defined in (27), be the set containing the equilibria of the closed-loop system (53). Then, from (28) the derivative of (61) satisfies

$$\dot{W}_\varsigma(\varsigma) \leq - \bar{c}'|\varsigma|_{\mathcal{W}_\varsigma}. \tag{65}$$

Thus, the closed-loop system (53) is uniformly asymptotically multi-stable at $\mathcal{W}_\varsigma$, cf. [19]. Furthermore, since the critical point $\tilde{z}_1^*$ of the barrier Lyapunov function is a saddle point, after [20, Prop. 1], it follows that the region of attraction of the unstable equilibrium $\tilde{z}_1^*$ has zero Lebesgue measure. Therefore, we conclude that the origin of (53) is *almost-everywhere* uniformly asymptotically stable in $\mathbb{D}$, except for a zero-measure set of initial conditions.

In order to establish forward invariance of the set $\tilde{\mathcal{D}}$ we proceed by contradiction. Assume that there exists $T > 0$ such that for all $t \in [0,T)$, $\tilde{z}_{1k}(t) \in \tilde{\mathcal{D}}_k$ and $z_{1k}(T) \notin \tilde{\mathcal{D}}_k$, for at least one $k \leq M$. More precisely, we have $|z_{1k}(t)| \to \Delta_k$ or $|z_{1k}(t)| \to \delta_k$ as $t \to T$ for at least one $k \leq M$. From the definition of $\tilde{z}_{1t} \mapsto W(\tilde{z}_{1t})$ in (26) and $\tilde{z}_{1k} \mapsto W_k(\tilde{z}_{1k})$ in (25), this implies that $W_\varsigma(\varsigma(t)) \to \infty$ as $t \to T$ which is in contradiction with (63). We conclude that $W_\varsigma(\varsigma(t))$ is bounded for all initial conditions such that $\tilde{z}_1(0) \in \tilde{\mathcal{D}}$, therefore, $W_\varsigma(\varsigma(t)) \leq W_\varsigma(\varsigma(0)) < \infty$ for all $\varsigma(0) \in \mathbb{D}$ and all $t \geq 0$. The respect of the inter-agent constraints follows from the forward invariance of $\tilde{\mathcal{D}}$.

Since (53) is asymptotically stable at the origin, with domain of attraction $\mathbb{D}$, it follows that for (almost) all initial conditions $\varsigma(0) \in \mathbb{D}$ there exist small positive constants $\underline{\epsilon}(\varsigma(0))$ and $\overline{\epsilon}(\varsigma(0))$ such that $\tilde{z}_{1k}(t) \in \tilde{\mathcal{D}}_{\epsilon k}$, where

$$\tilde{\mathcal{D}}_{\epsilon k} := \{\tilde{z}_{1k} \in \mathbb{R}^2 \,:\, \delta_k - \underline{\epsilon} \leq |\tilde{z}_{1k} + z_{1k}^d| \leq \Delta_k - \overline{\epsilon}\},\ \forall k \leq M.$$

Moreover, for any $\tilde{z}_1 \in \tilde{\mathcal{D}}_\epsilon$, with $\tilde{\mathcal{D}}_\epsilon := \bigcap_{k\leq M}\tilde{\mathcal{D}}_{\epsilon k}$, we have that the BLF W in (26) satisfies

$$\frac{a_1}{2}|\tilde{z}_{1t}|^2_{\mathcal{W}} \leq W(\tilde{z}_{1t}) \leq \frac{a_2'}{2}|\tilde{z}_{1t}|^2_{\mathcal{W}}. \tag{66}$$

Therefore, from (66) and (63), we conclude that for almost all initial conditions $\varsigma(0) \in \mathbb{D}$, the trajectories $\varsigma(t)$ of the external dynamics converge to the origin exponentially. ■

B. Boundedness of the internal dynamics

The interconnection term G in (47a) satisfies the bound

$$|G(\tilde{\zeta},\chi)| \leq G_1(|\chi|)|\tilde{\zeta}_s| + G_2(|\chi|), \tag{67}$$

where $G_1, G_2 \in \mathcal{K}$. Then, under the conditions (38), (40), (67), and Lemma 1, uniform ultimate boundedness of the trajectories of the internal dynamics (47a)-(47b) follows from the same arguments as in the proof of [13, Theorem 1]. This proof is omitted here due to space constraints. ■

V. Numerical Example

In this section we illustrate the performance of the controller (6), with (35), through a numerical example consisting of the tracking-in-formation problem for six ASVs subject to proximity and collision-avoidance constraints. It is only assumed that the vehicles are interconnected at the initial time, so the controller must preserve such connectivity. We consider that the agents interact over a connected undirected graph and that only the agent labeled ”1” has knowledge of the (relative) state of the target (labeled ”0”). The topology is illustrated in Fig. 2.

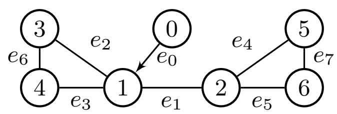

Fig. 2. Interaction topology: connected undirected graph.

The six ASVs are considered identical and correspond to the model of CybershipII [21], which is a scale model of an offshore supply vessel with mass 15 kg, length of 1.255 m, and whose mass and damping matrices are given by

$$M = \begin{bmatrix} 25.8 & 0 & 0 \\ 0 & 33.8 & 1.01 \\ 0 & 1.01 & 2.76 \end{bmatrix}, \; D = \begin{bmatrix} 0.93 & 0 & 0 \\ 0 & 2.89 & -0.26 \\ 0 & -0.26 & 0.5 \end{bmatrix}.$$

Moreover, the ocean current velocity is set to $\mathbf{V} = [V_x \;\; V_y]^\top = [0.05 \;\; -0.08]^\top$. The initial conditions of the agents are presented in Table I.

TABLE I
Initial conditions

Index	x_i	y_i	ψ_i	u_{ri}	v_{ri}	r_i
1	1.9	0	0	0.6	0.2	0
2	-2	0	0	0.3	0	0
3	5.5	2	$-\pi/2$	0.3	0.2	0
4	5.5	-2	$\pi/2$	0.3	0	0
5	-5.5	2	0	0	0.1	0
6	-5.5	-2	0	0.8	0	0

The desired formation corresponds to a hexagon determined by the relative position vector $z_{1k}^d = (z_{1k,x}^d, z_{1k,y}^d)$, for each $k \leq 5$, set to $(1, 0.5)$, $(-1, -1.5)$, $(-1, 0.5)$, $(-2, 1)$, $(-1, 0.5)$. The target is modeled as a second-order integrator (11) following a circular trajectory with the input

$$\mu_o(t) = [-0.018\cos(0.06t) \quad -0.018\sin(0.06t)]^\top,$$

and initial conditions $h_o(0) = [15 \quad 0]^\top$m and $\nu_{ho}(0) = [0 \;\; 0.3]^\top$m/s. The maximal and minimal distance parameters are $\Delta_k = 4.4$m and $\delta_k = 0.4$m. The hand position point is chosen at $l = 1$m, and the control gains are set to $c_1 = 1$, $c_2 = 0.5$, $\gamma = 0.15$, and $c_v = 0.2$. All the parameters and control gains are chosen so that the conditions (38)-(40) are satisfied. Furthermore, in order to avoid discontinuities in the control, the non-smooth term in (35) is replaced by the smooth approximation $-\gamma \tanh(c_a s)$, $c_a \gg 1$.

Fig. 3-6 present the results of the simulation scenario. We see from Fig. 3 that the ASVs successfully reach the desired formation while following the target, as is also evidenced from the formation and tracking errors in Fig. 5 and the velocity errors in Fig. 6. Furthermore, note that the connectivity and collision avoidance constraints, shown as dashed red lines in Fig. 4, are always respected. Thus, the simulation results successfully verify Theorem 1 and illustrate the performance of the proposed controller.

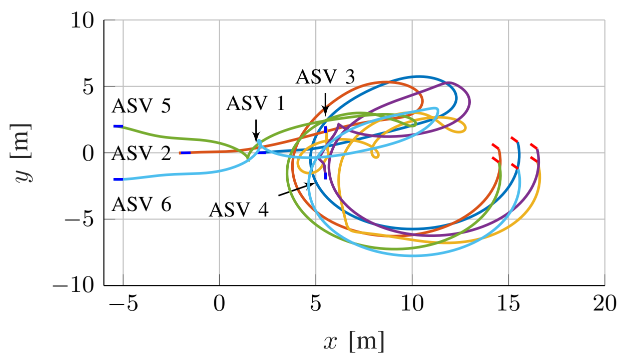

Fig. 3. Paths followed by the agents.

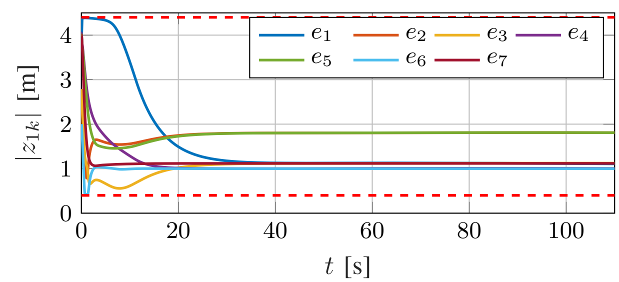

Fig. 4. Inter-agent distances. The dashed lines represent the connectivity and collision-avoidance constraints.

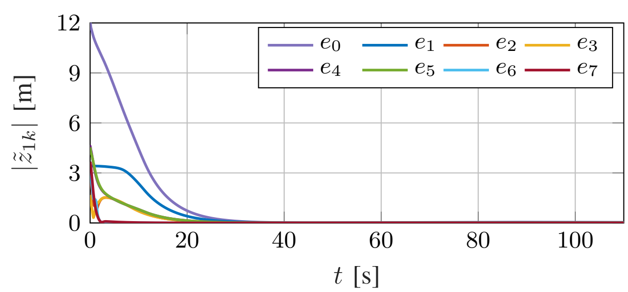

Fig. 5. Norms of the formation/tracking errors.

VI. Conclusions and Future Work

We presented a solution to the tracking-in-formation control problem of cooperative autonomous marine vehicles under inter-agent output constraints. Building upon an input-output feedback transformation we proposed a distributed controller, using the gradient of a BLF and a backstepping design, that achieves the desired formation and target

Manuscript 125 submitted to 2022 European Control Conference (ECC).
Received October 31, 2021.

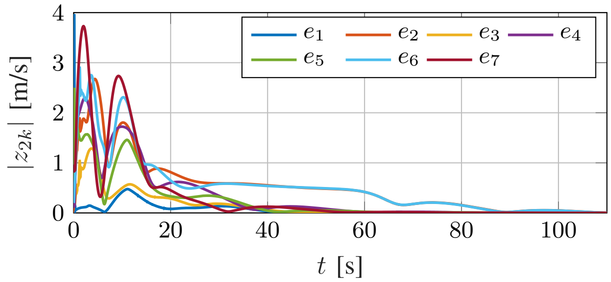

Fig. 6. Norms of the velocity errors.

tracking with guaranteed connectivity maintenance and inter-agent collision avoidance even in the presence of constant disturbances and with limited knowledge of the target. We established almost-everywhere uniform asymptotic stability with exponential convergence of the output dynamics. Current research focuses on extending these results to AUVs moving in 3D and considering input and velocity constraints.

Appendix I
Equations

Under Assumptions 1-3 the ASVs may be represented by a mass and a damping matrix of the form

$$M = \begin{bmatrix} m_{11} & 0 & 0 \\ 0 & m_{22} & m_{23} \\ 0 & m_{23} & m_{33} \end{bmatrix},\ D = \begin{bmatrix} d_{11} & 0 & 0 \\ 0 & d_{22} & d_{23} \\ 0 & d_{32} & d_{33} \end{bmatrix}.$$

Then, we have.

$$X_1 = \frac{m_{11}m_{33} - m_{23}^2}{m_{22}m_{33} - m_{23}^2};\ X_2 = \frac{d_{33}m_{23} - d_{23}m_{33}}{m_{22}m_{33} - m_{23}^2} \tag{68}$$

$$Y_1 = \frac{(m_{11} - m_{22})m_{23}}{m_{22}m_{33} - m_{23}^2};\ Y_2 = \frac{d_{22}m_{33} - d_{32}m_{23}}{m_{22}m_{33} - m_{23}^2} \tag{69}$$

$$F_{u_r}(v_r, r) = \frac{1}{m_{11}}(m_{22}v_r + m23r)r - \frac{d_{11}}{m_{11}}u_r \tag{70}$$

$$\begin{aligned} F_r(u_r, v_r, r) =& \frac{m_{23}d_{22} - m_{22}(d_{32} + (m_{22} - m_{11})u_r)}{m_{22}m_{33} - m_{23}^2}v_r \\ &+ \frac{m_{23}(d_{23} + m_{11}u_r) - m_{22}(d_{33} + m_{23}u_r)}{m_{22}m_{33} - m_{23}^2}r \end{aligned} \tag{71}$$

$$\begin{aligned} \alpha(\tilde{\zeta}_i, \bar{\xi}_{3i}, \bar{\xi}_{4i}) =& - \left[\frac{Y_1}{l}\left[(\bar{\xi}_{3i}\cos(\tilde{\zeta}_{1i} + \phi_o) + \bar{\xi}_{4i}\sin(\tilde{\zeta}_{1i} + \phi_o))\right.\right. \\ &\left.\left. + U_o\cos\tilde{\zeta}_{1i}\right] + \frac{Y_2}{l}\right]\sin(\tilde{\zeta}_{1i} + \phi_o) - \left[\frac{Y_1}{l}U_o\sin\tilde{\zeta}_{1i}\right. \\ &\left. + \left(Y_1 - \frac{X_1 - 1}{l}\right)\zeta_{2i}\right]\cos(\tilde{\zeta}_{1i} + \phi_o) \end{aligned} \tag{72}$$

$$\begin{aligned} \beta(\tilde{\zeta}_i, \bar{\xi}_{3i}, \bar{\xi}_{4i}) =& \left[\frac{Y_1}{l}\left[(\bar{\xi}_{3i}\cos(\tilde{\zeta}_{1i} + \phi_o) + \bar{\xi}_{4i}\sin(\tilde{\zeta}_{1i} + \phi_o))\right.\right. \\ &\left.\left. + U_o\cos\tilde{\zeta}_{1i}\right] + \frac{Y_2}{l}\right]\cos(\tilde{\zeta}_{1i} + \phi_o) - \left[\frac{Y_1}{l}U_o\sin\tilde{\zeta}_{1i}\right. \\ &\left. + \left(Y_1 - \frac{X_1 - 1}{l}\right)\zeta_{2i}\right]\sin(\tilde{\zeta}_{1i} + \phi_o) \end{aligned} \tag{73}$$

References

[1] J. Nicholson and A. Healey, "The present state of autonomous underwater vehicle (AUV) applications and technologies," *Marine Technology Society Journal*, vol. 42, no. 1, pp. 44–51, 2008.

[2] E. Borhaug and K. Y. Pettersen, "Formation control of 6-DOF Euler-Lagrange systems with restricted inter-vehicle communication," in *Proc. 45th IEEE Conf. Decision and Control*, 2006, pp. 5718–5723.

[3] R. Ghabcheloo, A. P. Aguiar, A. Pascoal, C. Silvestre, I. Kaminer, and J. Hespanha, "Coordinated path-following control of multiple underactuated autonomous vehicles in the presence of communication failures," in *Proc. 45th IEEE Conf. Decision and Control*, 2006, pp. 4345–4350.

[4] W. Zhang and J. Hu, "Optimal multi-agent coordination under tree formation constraints," *IEEE Trans. Autom. Control*, vol. 53, no. 3, pp. 692–705, 2008.

[5] R. Cui, S. Sam Ge, B. Voon Ee How, and Y. Sang Choo, "Leader–follower formation control of underactuated autonomous underwater vehicles," *Ocean Engineering*, vol. 37, no. 17, pp. 1491–1502, 2010.

[6] M. Soorki, H. Talebi, and S. Nikravesh, "A robust dynamic leader-follower formation control with active obstacle avoidance," in *Proc. 2011 IEEE International Conference on Systems, Man, and Cybernetics*, 2011, pp. 1932–1937.

[7] B. Das, B. Subudhi, and B. B. Pati, "Cooperative formation control of autonomous underwater vehicles: An overview," *International Journal of Automation and Computing*, vol. 13, no. 3, pp. 199–225, Jun. 2016.

[8] G. P. Roussos, D. V. Dimarogonas, and K. J. Kyriakopoulos, "3D navigation and collision avoidance for a non-holonomic vehicle," in *Proc. 2008 American Control Conference*, Jun. 2008, pp. 3512–3517.

[9] A. Mujumdar and R. Padhi, "Reactive collision avoidance using nonlinear geometric and differential geometric guidance," *Journal of Guidance, Control, and Dynamics*, vol. 34, no. 1, pp. 303–311, Jan. 2011.

[10] E. A. Basso, E. H. Thyri, K. Y. Pettersen, M. Breivik, and R. Skjetne, "Safety-Critical Control of Autonomous Surface Vehicles in the Presence of Ocean Currents," in *Proc. 4th IEEE Conference on Control Technology and Applications*, Aug. 2020, pp. 396–403.

[11] D. Zelazo, A. Rahmani, and M. Mesbahi, "Agreement via the edge Laplacian," in *Proc. 46th IEEE Conf. Decision and Control*, New Orleans, LA, USA, 2007, pp. 2309–2314.

[12] E. Restrepo, A. Loría, I. Sarras, and J. Marzat, "Stability and robustness of edge-agreement-based consensus protocols for undirected proximity graphs," *International Journal of Control*, pp. 1–9, 2020.

[13] C. Paliotta, E. Lefeber, K. Y. Pettersen, J. Pinto, M. Costa, and J. T. de Figueiredo Borges de Sousa, "Trajectory tracking and path following for underactuated marine vehicles," *IEEE Trans. Control Syst. Technol.*, vol. 27, no. 4, pp. 1423–1437, 2019.

[14] T. I. Fossen, *Handbook of marine craft hydrodynamics and motion control*. John Wiley & Sons, 2011.

[15] M. Ji and M. Egerstedt, "Distributed coordination control of multiagent systems while preserving connectedness," *IEEE Trans. Robot.*, vol. 23, no. 4, pp. 693–703, Aug. 2007.

[16] D. Boskos and D. V. Dimarogonas, "Robustness and invariance of connectivity maintenance control for multiagent systems," *SIAM J. on Control and Optimization*, vol. 55, no. 3, pp. 1887–1914, 2017.

[17] K. P. Tee, S. S. Ge, and E. H. Tay, "Barrier Lyapunov functions for the control of output-constrained nonlinear systems," *Automatica*, vol. 45, no. 4, pp. 918–927, 2009.

[18] E. Rimon and D. E. Koditschek, "Exact robot navigation using artificial potential functions," *IEEE Trans. Robot. Autom.*, vol. 8, no. 5, pp. 501–518, Oct. 1992.

[19] P. Forni and D. Angeli, "Input-to-state stability for cascade systems with multiple invariant sets," *Systems & Control Letters*, vol. 98, pp. 97–110, 2016.

[20] P. Monzón and R. Potrie, "Local and global aspects of almost global stability," in *Proc. 45th IEEE Conf. Decision and Control*, 2006, pp. 5120–5125.

[21] E. Fredriksen and K. Pettersen, "Global κ-exponential way-point maneuvering of ships: Theory and experiments," *Automatica*, vol. 42, no. 4, pp. 677–687, 2006.

Manuscript 125 submitted to 2022 European Control Conference (ECC).
Received October 31, 2021.